Account of mismatching effect based on constraint in welded joints and fracture toughness predication

Zhong-An Chen[1], Guang-Zhi Li [1], Yuh J. Chao [2], Jing Zeng [3]
[1,] *Jiangsu University, Zhenjiang, China*
[2] *University of South Carolina, Columbia, U.S.A*
[3] *Southwest Jiaotong University, Chengdu, China*

Abstract: Using finite element method, modified boundary layer model for homogeneous and heterogeneous welded joints are analyzed. After investigating the relationship of the opening stress at the crack tip in these two cases, a new constraint parameter is developed for overmatched welded joints, allowing the material mismatching effect on the crack tip stress to be quantified. The new constraint parameter is based on the $J-A_2$ three-term solution which is a reasonably good approach to describe the geometry constraint at the crack tip. In the case of complete specimens, constraint arising from both geometry and material mismatching exists. The total constraint has been obtained in establishing the relationship between A_2 and A_{2m} which is a new constraint parameter related to the mismatch. Finally, using the experimentally determined fracture toughness at one mismatch level, we predict the fracture toughness values at other mismatch levels. The result is consistent with the experiment data.

Keywords: crack tip constraint; welded joints; $J-A_2$ three-term solution; fracture toughness; mismatch effect

1. Introduction

The material strength mismatch existed between weld and base metal is an important consideration in safety assessment of welded components. Many experimental results [1, 2] indicate that the difference of material mismatch and geometry can cause different crack tip field state which greatly influences the fracture behavior of welded joints. Based on the traditional geometric constraint method such as $J-T$ [3], and $J-Q$ [4] approach, some researchers have considered material mismatch also as a constraint. Several formulations were developed in order to include the total constraint from both the geometry and mismatch [5,6]. These two approaches are however inaccurate under large scale yielding conditions that are often the case in actual welded steel structures. In this paper, a new parameter A_{2m} for material mismatch is proposed to add into the $J-A_2$ three term solution [7], which is the most accurate in LSY. Finally, the modified $J-A_2$ three term solution is validated through comparison with the fracture toughness values determined from experiment.

2. Separation of two types of constraint

2.1 The $J-A_2$ three term solution in homogenous materials

According to the theory of $J-A_2$ three term solution, the crack tip stress field of mode I crack for the hardening exponent $n \geq 3$ in a power law material can be written as:

$$\frac{\sigma_{ij}}{\sigma_s} = A_1\left[\left(\frac{r}{L}\right)^{S_1}\tilde{\sigma}_{ij}^{(1)}(\theta,n) + A_2\left(\frac{r}{L}\right)^{S_2}\tilde{\sigma}_{ij}^{(2)}(\theta,n) + A_2^2\left(\frac{r}{L}\right)^{S_3}\tilde{\sigma}_{ij}^{(3)}(\theta,n)\right] \qquad (1)$$

where $\tilde{\sigma}_{ij}^{(k)}(\theta)$ $(k=1,2,3)$ are the angular stress functions, S_k $(s_1 < s_2 < s_3)$ are the exponents of stress singularities that depend only on n, and $S_3 = 2S_2 - S_1$. L is a characteristic length parameter which can be chosen as 1 mm. The first term is the HRR field and is given by:

$$A_1 = \left(\frac{J}{\alpha\varepsilon_s\sigma_s I_n L}\right)^{-S_1} \qquad S_1 = -\frac{1}{n+1}$$

where the factor I_n only depends on the hardening exponent n. The values of $\tilde{\sigma}_{ij}^{(k)}(\theta)$ and S_k are tabulated in Ref. [8]. The constraint parameter A_2 can be determined by matching the opening stress form (Eq.1) with the finite element results at $r\sigma_s/J = (1\sim 2)$.

2.2 The modified boundary layer (MBL) model

In order to separate the effect of geometry from material mismatch on the stress fields, the MBL model is employed within the context of the finite element method. Fig. 1 shows the two models used. The first one, Fig. 1(a), models a weld material and a base material with the crack being contained in the centre of the weld material and run parallel to the weld/base interface. The second one, Fig. 1(b), models a homogeneous all weld material situation. In both cases the load is applied through displacements applied at the remote circular boundary, which are given by the elastic asymptotic stress field of plane strain mode I crack:

$$\begin{aligned} u_1 &= K_I\frac{(1+\nu)}{E}\sqrt{\frac{r}{2\pi}}(3-4\nu-\cos\theta)\cos\frac{\theta}{2} + T\frac{(1-\nu^2)}{E}r\cos\theta \\ u_2 &= K_I\frac{(1+\nu)}{E}\sqrt{\frac{r}{2\pi}}(3-4\nu-\cos\theta)\sin\frac{\theta}{2} - T\frac{(1+\nu)}{E}\nu r\sin\theta \end{aligned} \qquad (2)$$

where E is the Young's modulus of the material and ν is the Poisson's ratio, u_1 and u_2 are the displacements along the X and Y axis, r and θ are the polar co-ordinates centered at the crack tip.

The stress-strain relation follows the Ramberg-Osgood relation with E=200GPa, ν=0.3, and the hardening exponent n=10. Former research results indicate that in the case of undermatched weld the crack tip stress field is quite irregular [6]. Therefore, only overmatched case is considered here which is typical for steel weldment. The yield strength of the weld metal is σ_{ow}=625MPa. The mismatch ratios $m = \sigma_{ow}/\sigma_{ob}$ considered in this work are 1.1, 1.2, 1.3, 1.4, 1.5, and 1.6

which correspond to 568.2MPa, 520.8 MPa, 480.8 MPa, 446.4 MPa, 416.7 MPa, and 390.6 MPa of the yield strength of the base metal σ_{ob}.

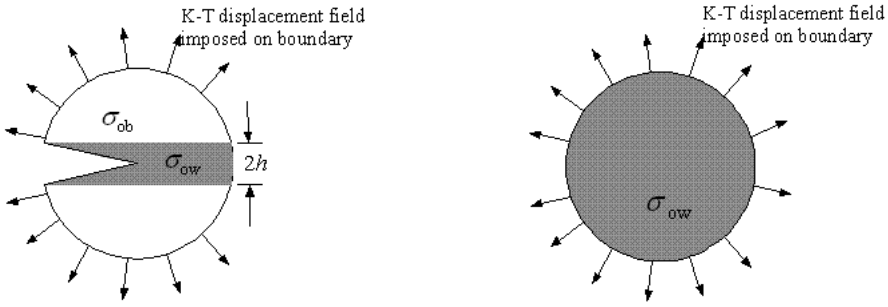

(a) mismatched (b) all weld

Fig. 1 Boundary layer geometries model

The ABAQUS finite element code is used to analyze the models shown in Fig.1. A typical finite element mesh is shown in Fig.2. The mesh represents one-half of the specimens since symmetry has been applied. All the meshes have an outer boundary radius of 500 mm and the radius of the notch tip is 0.005 mm. Plane strain conditions are considered and eight-node plane strain; second order isoperimetric elements are used.

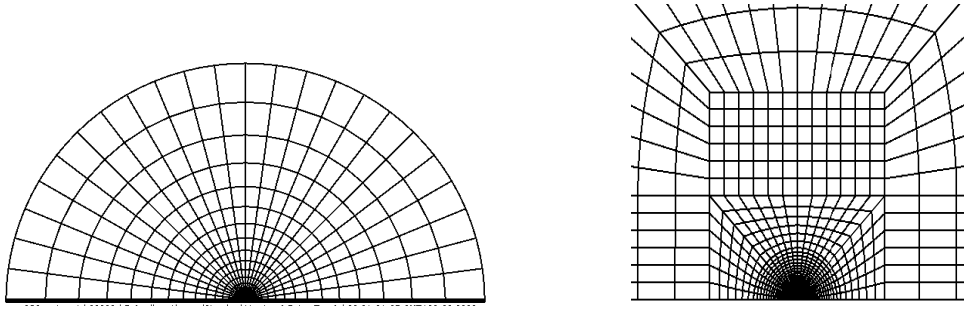

（a） general mesh (b) The crack tip region mesh

Fig. 2 Mesh for the boundary layer models

In the model of mismatched weld, shown in Fig.1(a), the T term in the applied displacements (Eq. 2) is equal to zero, and therefore constraint is only due to material mismatch. In all weld model of Fig.1(b), different value of geometry constraint is obtained by varying the value of T stress. So the two models correspond to the cases of only material constraint and only geometry constraint, respectively.

2.3 Results of modified boundary layer model

For the model shown in Fig. 1(a), the development of the crack tip opening stress at a fixed distance ahead of the crack tip, i.e. $r\sigma_{ow}/J = 2$, from different mismatch is shown in Fig. 3. In the calculation, the width of the weld h is kept constant, while altering the values of J - integral to represent the load level. The non-mismatched state $m = 1$ is chosen as a reference case.

We can see from the graph that at the same load level, the larger the mismatch ratio m is, the larger the effect of constraint loss corresponding to lower crack tip opening stress compared with the reference stress. In addition, at the same mismatch ratio m, the constraint loss is more severe as the load J increases.

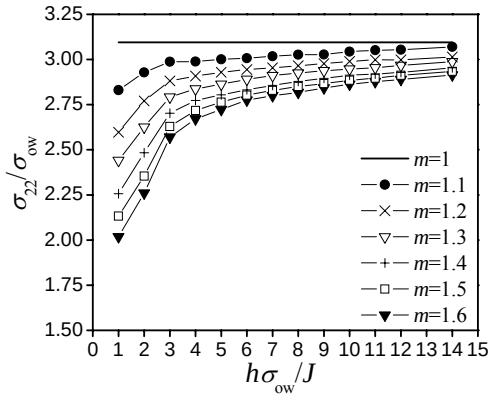

Fig. 3 Normalized opening stress at $r\sigma_{ow}/J = 2$ as a function of the load level for different mismatch ratios m

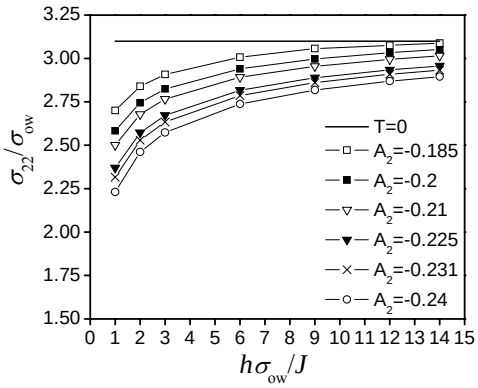

Fig. 4 Normalized opening stress at $r\sigma_{ow}/J = 2$ as a function of the load level for different geometry constraint, obtained from homogenous modified boundary layer model.

Similarly, for the all weld model shown in Fig. 1(b), the value of the parameter A_2 corresponding to the different geometry constraint is obtained and the development of the crack tip opening stress with the load is shown in Fig. 4 for different T, which corresponding to different A_2, The $T = 0$ case is chosen as a reference case.

We can also see from Fig.4 that at the same load level, lower A_2 yields greater geometry constraint and lower opening stress compared with the reference state. In addition, at the same A_2, the larger load or J yields more severe geometry

constraint loss.

3. The modified $J - A_2$ three term solution for welded structure

3.1 The mismatch constraint parameter A_{2m}

Results in Figs 3 and 4 demonstrate that similar behavior exists between the welded joints with $T = 0$, where constraint is only due to material mismatch, and those of homogeneous materials with different values of the constraint parameter A_2, where the constraint loss is only due to geometry.

By comparing Figs. 3 and 4, at each load level $h\sigma_{ow}/J$, one seeks out the stress corresponding to each mismatching ratio m from Fig.3, find the value of A_2 corresponding to this stress value from Fig.4, then, a relation between m and A_2 can be found. Fig.5 shows these results where the solid line is the fitted curve given as

$$A_2 = -0.4m^3 + 1.79m^2 - 2.72m + 1.18 \tag{3}$$

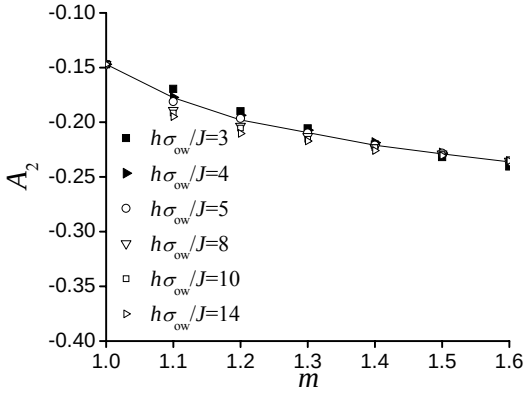

Fig. 5 Mismatch ratio and geometry constraint relationship

With the relation in Eq. (3), one can define a mismatch constraint parameter A_{2m} to scale the effect of constraint due to mismatch. Eq. (3) now becomes

$$A_{2m} = -0.4m^3 + 1.79m^2 - 2.72m + 1.03 \tag{4}$$

Note that when $m = 1$ (no mismatch) $A_2 = -0.15$, the constant term in Eq. (3), i.e. 1.18, is adjusted to 1.03 in Eq. (4) to reflect this observation. Eq. (4) indicates that the constraint level for each mismatched weld of ratio m in a weld can be uniquely determined by the value of A_{2m} .

In specimens or structures, both geometry constraint and material mismatch are present. As both decrease the stress field as shown in Figs 3 and 4, so the total constraint can be $A_2 + A_{2m}$. In other words, in a weld structure the crack tip stress field of power-law hardening material in mode I case can be expressed as:

$$\frac{\sigma_{ij}}{\sigma_s} = A_1\left[\left(\frac{r}{L}\right)^{S_1}\tilde{\sigma}_{ij}^{(1)}(\theta,n)+\left(A_{2m}+A_2\right)\left(\frac{r}{L}\right)^{S_2}\tilde{\sigma}_{ij}^{(2)}(\theta,n)+\left(A_{2m}+A_2\right)^2\left(\frac{r}{L}\right)^{S_3}\tilde{\sigma}_{ij}^{(3)}(\theta,n)\right] \tag{5}$$

Eq. (5) is the modified $J-A_2$ solution in welded structure. A_{2m} is a function of the mismatch of the weld and be obtained from Eq. (4). Other parameters are from homogeneous materials as discussed in 2.1.

3.2 Application of the modified solution

In homogeneous material, the $J-A_2$ solution is valid in both small scale yielding (SSY) and large scale yielding (LSY). But in welded structure, the mismatching constraint A_{2m} exist (see Eq(5)), so we must first analyze its validity to characterize the crack tip stress fields. To do this, two three-point bend specimens with $a/w=0.15$ and $a/w=0.5$ with a weld strip of width $2h$ located in the center of the specimen were analyzed using the finite element method (FEM).

Fig.6 shows the finite element results of the crack tip opening stress ahead of the crack tip. It can be seen that, at the load level shown in Fig.6, the stress predicted by the modified $J-A_2$ solution agree better than those by the $J-A_2$ solution alone, as compared with those from FEM.

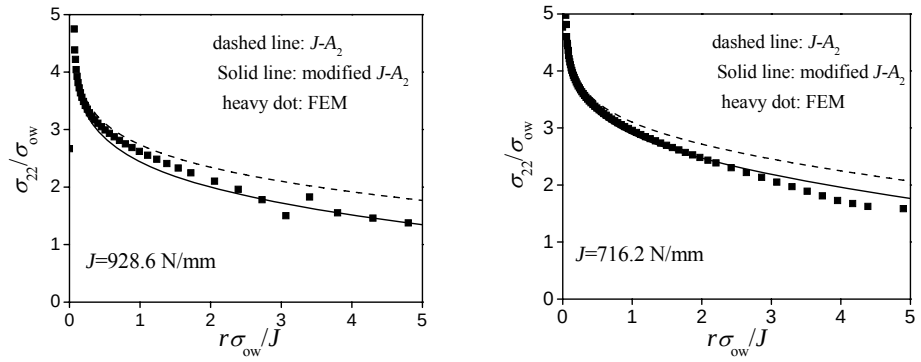

(a) $a/w=0.15,\ m=1.4$ (b) $a/w=0.5,\ m=1.4$

Fig. 6 Comparison the crack tip fields of $J-A_2$ solution, modified $J-A_2$ solution and FEM.

Fig.7 shows the crack tip opening stress at various load level for the configuration $m=1.6$ and $a/w=0.15$, which the constraint losses due to both geometry and material mismatch are maximum. In $a\sigma_{ow}/J$, the crack tip a is kept constant, while altering the values of J- integral to represent the load level. If one establishes an error formula as

$$\text{Error} = \left[\left(\frac{\sigma_{22}}{\sigma_{\text{ow}}} \right)_{\text{FEM}} - \left(\frac{\sigma_{22}}{\sigma_{\text{ow}}} \right)_{J-A_2} \right] \Bigg/ \left(\frac{\sigma_{22}}{\sigma_{\text{ow}}} \right)_{\text{FEM}} \times 100\% \le 5\%$$

It can be seen from Fig 7 that the modified $J - A_2$ solution has an error within 5% in the range of $a\sigma_{ow}/J \in (10,120)$. Note that the load range encompasses both SSY and LSY in Fig 7. It is then concluded that the modified $J - A_2$ solution can well predict the crack tip stress field of general welded specimen in both SSY and LSY.

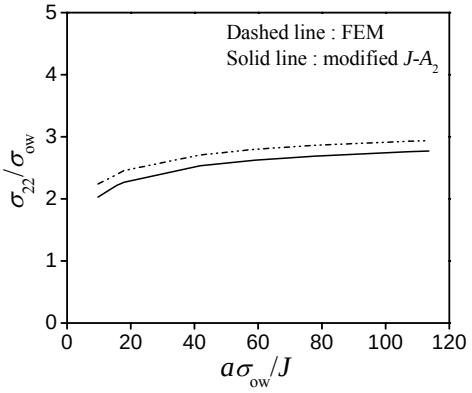

Fig. 7 Comparison of the opening stress at $r\sigma_{\text{ow}}/J = 2$: modified $J - A_2$ results with finite element solutions

4 The constraint -modified $J - R$ curves of welded structure

Cracks in ductile materials may exhibit $J - R$ curve behavior. Here the modified $J - A_2$ three-term solution is used to modify the $J - R$ resistance curves for welded structure.

Fig.8 contains the $J - R$ resistance curves obtained from Ref.[9], The $J - R$ resistance curve of the 1, 2, 3, 4 in Fig.8 is $J_R = 800.61(\Delta a)^{0.583}$, $J_R = 488.84(\Delta a)^{0.515}$, $J_R = 444.25(\Delta a)^{0.528}$, and $J_R = 393.43(\Delta a)^{0.567}$. Extending the *J-R* curve to include the constraint A_2, one has [10]

$$J(\Delta a, A_2) = C_1(A_2)\left(\frac{\Delta a}{k} \right)^{C_2(A_2)}$$

The coefficients $C_1(A_2)$, $C_2(A_2)$ are unknown and depend upon the constraint A_2 at the crack tip for a specific material and specimen, and $k = 1.0\text{mm}$. In modified $J - A_2$ method for welds, the only difference is that geometry constraint A_2 now becomes the total constraint $A_2 + A_{2m}$. Or, the $J - R$ resistance curve of welded specimen is expressed as

$$J(\Delta a, A_2 + A_{2m}) = C_1(A_2 + A_{2m})(\Delta a)^{C_2(A_2 + A_{2m})} \tag{6}$$

Applying the method discussed in section 3.1, the total constraint A_2+A_{2m} of the four cases in Fig. 8 are -0.377, -0.324, -0.314, -0.261 respectively.

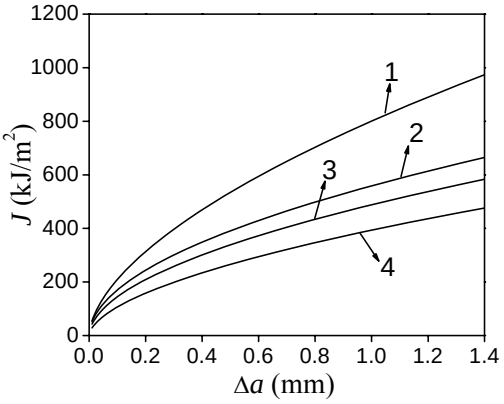

Fig. 8 Resistance curves of welded specimens at different material mismatch *m* and different crack length. 1. $a/w=0.2$ $m=1.6$ 2. $a/w=0.2$ $m=1$, 3. $a/w=0.5$ $m=1.6$ 4. $a/w=0.5$ $m=1$.

To calculate the expression of $C_1\left(A_2+A_{2m}\right)$, $C_2\left(A_2+A_{2m}\right)$, using J integral under the case of Δa=0.2mm, Δa =1.0mm, the unknown value $C_1\left(A_2+A_{2m}\right)$ and $C_2\left(A_2+A_{2m}\right)$ can be obtained from the following two equations:

$$J_{0.2mm}=J_{0.2mm}\left(A_2+A_{2m}\right)=C_1\left(A_2+A_{2m}\right)\left(0.2\right)^{C_2\left(A_2+A_{2m}\right)} \tag{7}$$

$$J_{1.0mm}=J_{1.0mm}\left(A_2+A_{2m}\right)=C_1\left(A_2+A_{2m}\right)\left(1.0\right)^{C_2\left(A_2+A_{2m}\right)} \tag{8}$$

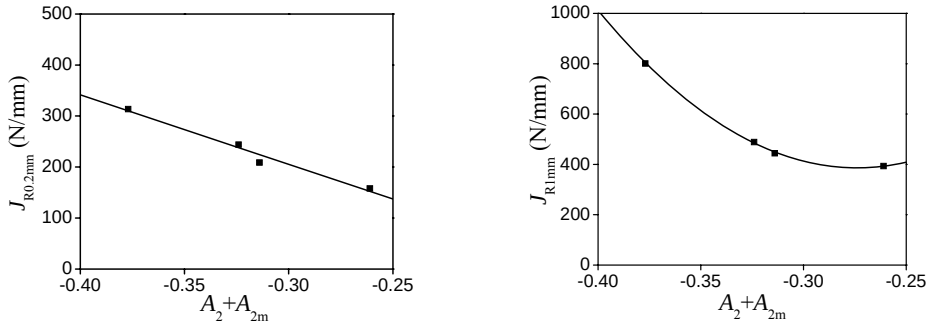

(a) (b)

Fig. 9 Total constraint and corresponding $J_{R0.2mm}$ and J_{R1mm} value

For the four cases shown in Fig.8, we obtained the corresponding relationships between $J_{R0.2mm}$ and A_2+A_{2m}, J_{R1mm} and A_2+A_{2m} and are shown in Fig.9 (a) (b), The solid line is from the fitting result as follows:

$$J_{R0.2mm}=-1362\left(A_2+A_{2m}\right)-203.4 \tag{9}$$

$$J_{R1mm} = 39387\left(A_2 + A_{2m}\right)^2 + 21581\left(A_2 + A_{2m}\right) + 3343 \tag{10}$$

Substituting the result of (9) (10) into (7) (8), another two expressions are obtained as

$$C_1\left(A_2 + A_{2m}\right)(0.2)^{C_2\left(A_2 + A_{2m}\right)} = -1362\left(A_2 + A_{2m}\right) - 203.4 \tag{11}$$

$$C_2\left(A_2 + A_{2m}\right)(1.0)^{C_2\left(A_2 + A_{2m}\right)} = 39387\left(A_2 + A_{2m}\right)^2 + 21581\left(A_2 + A_{2m}\right) + 3343 \tag{12}$$

$C_1\left(A_2 + A_{2m}\right)$, $C_2\left(A_2 + A_{2m}\right)$ can be determined from formulae (11) and (12):

$$C_1\left(A_2 + A_{2m}\right) = 39387\left(A_2 + A_{2m}\right)^2 + 21581\left(A_2 + A_{2m}\right) + 3343 \tag{13}$$

$$C_2\left(A_2 + A_{2m}\right) = 93.2\left(A_2 + A_{2m}\right)^2 + 59.6\left(A_2 + A_{2m}\right) + 9.9 \tag{14}$$

Substituting (13) and (14) into formula (6), finally the modified $J-R$ curve which contains both constraints from geometry and mismatch is then obtained as

$$J\left(\Delta a, A_2 + A_{2m}\right) = \Big[39387\left(A_2 + A_{2m}\right)^2 + 21581\left(A_2 + A_{2m}\right) + 3343\Big]\left(\Delta a\right)^{\left[93.2\left(A_2 + A_{2m}\right)^2 + 59.6\left(A_2 + A_{2m}\right) + 9.9\right]} \tag{15}$$

Eq. (15) is the predicted formula for $J-R$ curves of the welded specimen of Ref [9]. For welded specimens of the same materials but at other constraint level, once the total constraint is known, its $J-R$ curve can then be predicted using Eq(15).

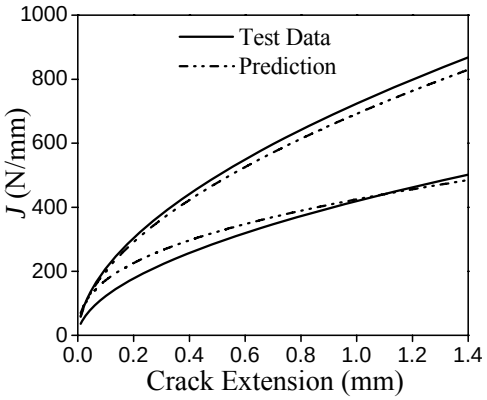

Fig. 10 Comparisons of $J-R$ curves between experimental data and the prediction by Eq 15.

The experimental $J-R$ curves of m =1.4, a/w =0.5 and m =1.4, a/w =0.24 from Ref.[9] are reported as $J_R = 419.42\left(\Delta a\right)^{0.534}$ and $J_R = 723.78\left(\Delta a\right)^{0.540}$ respectively. The predicted results according to Eq.15 are $J_R = 424.77\left(\Delta a\right)^{0.392}$ and $J_R = 692.10\left(\Delta a\right)^{0.538}$ respectively. Comparison between the experimentally determined *J-R* curve [9] and the prediction using Eq. 15 is shown in Fig.10 which shows a good agreement.

5. Conclusion

A mismatch constraint parameter A_{2m} is defined and developed in this paper. By

using this parameter, $J-A_2$ three-term solution of homogeneous material is extended to the welded material having material mismatch. The constraint in the $J-A_2$ three-term solution now includes both effects from the material mismatch and geometry. The modified $J-R$ curves obtained from the modified $J-A_2$ three-term solution are also able to predict the $J-R$ curves of other specimens made of the same material or other mismatching ratio. The procedure provides a useful methodology in dealing with the fracture in welded joints when material mismatch is present.

Acknowledgment
The work is sponsored by the Opening Fund of Traction Power State Key Laboratory of Southwest Jiaotong University (1721190059). The support is greatly appreciated.

References

[1] F. Minani, M. Ohata, M. Toyoda, Determination of required toughness of materials considering transferability to fracture performance evaluation for structure components. Journal of the Society of Naval Architects of Japan 182(1997) 647-657
[2] C. Betegon, J.W. Hancock, Two parameter characterization of elastic-plastic crack-tip fields. ASME Journal of Applied Mechanics 58 (1991)104-110
[3] N.P. O'Doud, C.F. Shih, Two parameter fracture mechanics: Theory and Application. American Society for Testing and Materials, Philadelphia 24 (1994) 41-63
[4] Z. L. Zhang, M. Hauge, C. Thaulow, Two-parameter characterization of the near tip stress fields for a bi-material elastic-plastic interface crack. International Journal Fracture 79 (1996)65-83
[5] M.C. Burstow, I.C. Howard, R.A. Ainsworth, The influence of constraint on crack tip stress fields in strength mismatched welded joints. Journal of the Mechanics and Physics of Solids 46 (1998)845–872
[6] C. Betegón, I. Peñuelas, A constraint based parameter for quantifying the crack tip stress fields in welded joints. Engineering Fracture Mechanics 73 (2006) 1865–1877
[7] Y.J. Chao, S. Yang, M.A. Sutton, On the fracture of solids characterized by one or two Parameters: theory and practice. Journal of the Mechanics and Physics of Solids 42 (1994)629-647
[8] Y.J. Chao, L. Zhang, Tables of plane strain crack tip fields: HRR and higher order terms ,me report, Columbia: University of South Carolina (1997)97-1[R].
[9] I. Peñuelas, C. Betegón, C. Rodríguez, A ductile failure model applied to the determination of the fracture toughness of welded joints. Numerical simulation and experimental validation. Engineering Fracture Mechanics 73 (2006)2756-2773
[10] Y.J. Chao, X.K. Zhu, Constraint-modified *J-R* curves and its application to ductile crack growth. International Journal of Fracture 106 (2000) 135-160